



HAL
open science

Inference procedures to estimate potential based movement models in ecology

Pierre Gloaguen, Marie-Pierre Etienne, Sylvain Le Corff

► **To cite this version:**

Pierre Gloaguen, Marie-Pierre Etienne, Sylvain Le Corff. Inference procedures to estimate potential based movement models in ecology. 2015. hal-01207001v2

HAL Id: hal-01207001

<https://hal.science/hal-01207001v2>

Preprint submitted on 18 Nov 2016 (v2), last revised 20 Sep 2017 (v3)

HAL is a multi-disciplinary open access archive for the deposit and dissemination of scientific research documents, whether they are published or not. The documents may come from teaching and research institutions in France or abroad, or from public or private research centers.

L'archive ouverte pluridisciplinaire **HAL**, est destinée au dépôt et à la diffusion de documents scientifiques de niveau recherche, publiés ou non, émanant des établissements d'enseignement et de recherche français ou étrangers, des laboratoires publics ou privés.

Inference procedures to estimate potential based movement models in ecology

Pierre Gloaguen^{*1,2}, Marie-Pierre Etienne¹, and Sylvain Le Corff³

¹AgroParistech/INRA, UMR MIA 518, F-75231 Paris, France.

²Laboratoire Ecologie et Modèles pour l’halieutique, IFREMER, 44000, Nantes, France.

³Laboratoire de Mathématiques d’Orsay, Univ. Paris-Sud, CNRS, Université Paris-Saclay, Orsay, France.

Abstract

This paper proposes a statistical analysis of movement data in ecology using partially observed stochastic differential equations. Usually, in movement ecology, parameters of these models are estimated using approximate maximum likelihood procedures based on the Euler-Maruyama discretization. However, GPS sampling rate in ecology might not be large enough to ensure the stability and convergence of the Euler based estimates. To our best knowledge, there is no practical study to assess the performance of the Euler Maruyama method to estimate movement ecology models compared to other inference procedures for stochastic differential equations. In this paper, we propose such a practical study by comparing the Euler method with the Ozaki linearization method of [27, 30], an adaptive Kessler high order Gaussian approximation method introduced in [24, 25, 34], and the Exact Algorithm based Monte Carlo Expectation Maximization approach of [4]. The performance of these methods are assessed using a new potential based stochastic differential equation where the drift is given as the gradient of a mixture of attractive zones, which are of main interest in ecology and fisheries science. It is shown both on simulated data and actual fishing vessels data that the Euler method performs worse than the other procedures for non high frequency sampling schemes. We also show, on this model, that Kessler and Ozaki methods are quite robust and perform in a similar way as the exact method.

Keywords: Movement model; GPS data; Stochastic differential equation; Exact simulation; Local linearization; Pseudo Likelihood Methods.

1 Introduction

In ecology, statistical inference of animal movement models provide many insights on the ecological features that explain population-level dynamics. These analyses are crucial to wildlife managers to understand complex animal behaviors [17]. In fisheries science, understanding the underlying patterns responsible for spatial use of the ocean is a key aspect of a sustainable management [16]. Both fields promote now large programs to deploy Global Positioning

*Corresponding author: pierre.gloaguen@agroparistech.fr

System (GPS) device. For instance, we might mention, among others, the Tagging of Pelagic Predators program (TOPP, www.gtopp.org) or the TORSOOI (www.torsooi.com) program for marine animals and the WOLF GPS (www.wolfgps.com) or Elephant without Borders (www.elephantwithoutborders.org/tracking.php) programs for terrestrial wildlife. In the European Union, since the 1st of January 2012, fishing vessels above 12m are mandatory equipped with a Vessel Monitoring System which has become a standard tool of fisheries monitoring worldwide. As a result such programs produce large amount of trajectory data. These data sets have been largely used to understand, explain and potentially predict animals/vessels movements. The GPS-type loggers can be set with several acquisition frequencies which should be adjusted to the experimental setting. The chosen frequency is a crucial parameter to monitor animal behaviors over a given time horizon since GPS batteries highly depends on the number of recorded relocations. Relocations recordings are mostly set up at regular time steps between observations but real life experiments in complex environments (water for marine mammals for instance) might result in potentially strongly irregular time step acquisitions.

In many cases, the temporal resolution and the number of observations are sufficiently high to propose statistical learning procedures and to consider complex models estimation problems [8]. In the last few years, growing attention has been dedicated to continuous time and continuous space Markovian models as a realistic and flexible framework to model such data, [9, 12, 28]. These papers introduced stochastic differential equations (SDE) to describe and analyze animal trajectories. Since the model based on a pure diffusion process introduced in [32], a large variety of SDE have been proposed to model wildlife behavior, see [28] for references about elephant-seal migrations or trajectories of birds heading to a target for instance. This paper focuses on SDE based on a potential surface to capture the directional bias in animal patterns. As discussed in [13] this potential function is assumed to reflect the attractiveness of the environment and regions where species are likely to travel to. In the framework proposed by [11], the drift of the SDE is given by the gradient of a potential map P_η which depends on an unknown parameter η while the diffusion coefficient is a smooth function. This flexible framework has been widely used in movement ecology for the last 20 years, [9, 12, 13, 15, 21, 28, 29]. In [9, 10, 21] the authors introduced a quadratic potential function which means that the animal position is modeled by a bivariate Ornstein Uhlenbeck process. This is a convenient framework to represent attractiveness of a given area but it remains restrictive as animals are not prone to revert to a single attractive zone. The Ornstein Uhlenbeck process has also been used in movement ecology to model the velocity of an individual [23]. The popularity of such processes is explained by the fact that in this case the position is a Gaussian process with an explicit transition density and, therefore, the computation of the maximum likelihood estimator of η and the diffusion coefficient is straightforward. More complex potential functions have been proposed to model different animal behaviors [29] (including multiple attractive regions).

In this paper, we propose a model where the potential function is a mixture of Gaussian shaped functions. Potentials given by a mixture of parametric functions have been proposed in [29] but the model introduced in this paper is more general. Each attractive region is modeled by a mean location and an information matrix characterizing its dispersion while in [29] Gaussian potentials do not include correlation between coordinates. Therefore, the drift of the SDE is a mixture of Gaussian shaped functions, with unknown weights, centers and information matrices and represents the attractive regions where the species/fishing vessels are likely to travel. Designing efficient procedures to estimate the parameter η and the diffusion coefficient is a very challenging task in this setting as some basic properties of such models, such as transition probabilities, are usually not available in closed form.

Different statistical methods have been proposed to perform maximum likelihood esti-

mation in this framework, [22, 25]. The most convenient procedures to estimate discretely observed diffusion processes rely on discretization schemes to approximate the SDE between two observations and use a surrogate of the likelihood function to compute an approximate maximum likelihood estimator of η . The simplest likelihood approximation is obtained by the Euler-Maruyama method which replaces the drift and diffusion coefficients by their initial values on each interval. This may obviously be refined using a second order Milstein scheme for instance. A particularly interesting higher order scheme is given by the Ozaki discretization which proposes a linear approximation of the drift coefficient combined with a constant approximation of the diffusion term [27, 30]. More recently, [24], [25] and [34] introduced another Gaussian based approximation of the transition density between two consecutive observations using higher order expansions of the posterior mean and variance of an observation given the observation at the previous time step. Another approach for likelihood approximation based on Hermite polynomials expansion was introduced by [1, 2, 3] and extended in several directions recently, see [26] and all the references therein. To avoid the systematic bias associated with every discretization procedure which vanishes only when the number of discretization steps grows to infinity, [4] and [7] proposed to draw samples from finite-dimensional distributions of potential based diffusion processes. This sampling procedure is based on a rejection sampling procedure and may be used to sample from any finite dimensional distribution of the target SDE. This is a pivotal step to obtain an unbiased estimate of the intermediate quantity involved in an Expectation Maximization algorithm developed by these authors. As a by product this allows to sample trajectories exactly distributed according to the estimated model which is not possible with the three other methods.

To the best of our knowledge, in all published articles about movement ecology, the Euler-Maruyama method is used to estimate all parameters. The maximum likelihood estimator associated with this method and other discretization schemes may be proved to be consistent under some assumptions on the total number of observations n and the timestep Δ_n between observations (which is assumed to vanish to zero as n goes to infinity). However, as pointed out before, there is no guarantee that using GPS tagging in ecology would provide observations at a sufficiently high sampling rate which might result in an estimator suffering from a large bias, in particular with sparse observations. This bias may be reduced using higher order schemes as described above with an increasing computational complexity. On the other hand, Monte Carlo based exact algorithms introduced in [4, 7] may be used to obtain unbiased likelihood estimation so that the estimation error depends only on the number of simulations. However, the acceptance rejection step of these exact algorithms required to sample skeletons between each pair of observations has a computational complexity which grows with the timestep between observations. There is no theoretical nor practical studies to choose the method which achieves the best trade off between fast convergence and accuracy in movement ecology. In this work, we investigate the performance of four different methods, namely:

- the Euler-Maruyama method, described before, that is used in movement ecology ;
- the Ozaki local linearization method, proposed in [27] and [30] ;
- the Kessler high order Gaussian approximation method, proposed in [24] and refined using an adaptive procedure in [34] ;
- the Exact Algorithm based Monte Carlo EM method, proposed in [6].

The first three methods rely on a pseudo likelihood approach while the last method uses an Expectation Maximization (EM) algorithm to maximise the likelihood [18].

The paper is organized as follows. In Section 1, the potential based model framework of [11] is introduced along with the data this paper focuses on. This section also explains the maximum likelihood framework considered and the aforementioned methods used to produce parameter estimates. In section 3, a new movement ecology model which links attractive zones and trajectories is presented. Section 3.2 presents a simulation study to evaluate the robustness of the presented statistical methods with the specific potential function proposed here. In order to evaluate the impact of the sampling rate, three sampling scenarios are considered, high frequency, intermediate frequency, and low frequency. Finally, section 3.2 present an application of these three methods in order to estimate, from their positions, the attractive zones for two different French fishing vessels.

2 Presentation of the competing methods

In this paper, the animal or vessel position is assumed to be a stochastic process $(X_t)_{0 \leq t \leq T}$ defined on a probability space $(\Omega, \mathcal{F}, \mathbb{P})$ and taking values in \mathbb{R}^2 where T is a fixed time horizon. \mathbb{C} denotes the Wiener space defined as the set of continuous maps from $[0, T]$ to \mathbb{R}^2 endowed with the usual σ -algebra \mathcal{C} generated by cylinders. Let \mathbb{W}_T be the unique measure on the Wiener space such that the coordinate process $(\mathbf{W}_t)_{0 \leq t \leq T}$ is a standard Brownian motion on \mathbb{R}^2 associated with its natural filtration $\{\mathcal{F}_t\}_{0 \leq t \leq T}$. $(\mathbf{X}_t)_{0 \leq t \leq T}$ is assumed to be a solution to the following homogeneous SDE:

$$\mathbf{X}_0 = \mathbf{x}_0^g \quad \text{and} \quad d\mathbf{X}_t = b_\eta(\mathbf{X}_t)dt + \sigma_\gamma(\mathbf{X}_t)d\mathbf{W}_t \quad , \quad (1)$$

where $\eta \in \mathbb{R}^d$ and $\gamma \in \mathbb{R}^m$ are unknown parameters and $b_\eta : \mathbb{R}^2 \rightarrow \mathbb{R}^2$ and $\sigma_\gamma : \mathbb{R}^2 \rightarrow \mathbb{R}^2 \times \mathbb{R}^2$ are respectively the drift and the diffusion functions. Following [9, 13, 12, 28, 11, 14, 29, 21], it is assumed that the drift function b_η is defined as the gradient of a potential function $P_\eta : \mathbb{R}^2 \rightarrow \mathbb{R}$ and that σ_γ is constant: $\gamma \in \mathbb{R}$ and for all $x \in \mathbb{R}^2$,

$$b_\eta := \nabla P_\eta \quad \text{and} \quad \sigma_\gamma(x) = \gamma \quad . \quad (2)$$

Those gradient based movement models have been widely studied in ecology for the last 20 years. Two popular SDE based models in movement ecology are:

- the Brownian motion, with or without drift, corresponding to a constant b_η (that is a linear potential P_η), as in [32] ;
- the Ornstein Uhlenbeck process, corresponding to a linear drift function b_η (i.e a quadratic form for the potential P_η), as in [9].

These two models are appealing as their transition density function is available explicitly but lead to a very restricted class of potential functions P_η that might be unrealistic in real life learning applications. As an alternative to such popular models, a potential based on a mixture of Gaussian shaped functions is proposed and analyzed in Section 3.2. This mixture model is very flexible and can describe a wide range of situations by increasing the number of mixture components. The aim of this paper is to compare several maximum likelihood inference procedures to estimate the parameter $\theta = (\eta, \gamma)$ using a set of discrete time observations. These observations are given by G independent trajectories of an individual $\mathbf{x} = (\mathbf{x}^g)_{g=1, \dots, G}$ where each trajectory \mathbf{x}^g is made of $n_g + 1$ exact observations at times $t_0^g = 0 < t_1^g < \dots < t_{n_g}^g = T^g$ and starting at \mathbf{x}_0^g . The probability density of the distribution of \mathbf{X}_Δ given \mathbf{X}_0 is denoted by q_θ^Δ when the model is parameterized by θ : for all bounded measurable function h on \mathbb{R}^2 :

$$\mathbb{E}_\theta [h(\mathbf{X}_\Delta) | \mathbf{X}_0] = \int h(y) q_\theta^\Delta(\mathbf{X}_0, y) dy \quad ,$$

where \mathbb{E}_θ is the expectation when the model is driven by θ . As the G trajectories $(\mathbf{x}^g)_{g=1,\dots,G}$ are independent, the likelihood function may be written:

$$L(\theta; \mathbf{x}) = \prod_{g=1}^G \prod_{i=0}^{n^g-1} q_\theta^{\Delta_i^g}(\mathbf{x}_i^g, \mathbf{x}_{i+1}^g) \quad , \quad (3)$$

where $\Delta_i^g := t_{i+1}^g - t_i^g$. The maximum likelihood estimator of θ is defined as:

$$\hat{\theta} := \operatorname{argmax}_\theta L(\theta; \mathbf{x}) \quad .$$

In the cases of the Brownian motion and Ornstein Uhlenbeck processes, the function q_θ^Δ is the probability density function of a Gaussian random variable with known mean and covariance so that direct computation of $\hat{\theta}$ is an easy task. However, in more general settings such as in the model considered in Section 3.2, q_θ^Δ is unknown, making impossible the direct computation of $\hat{\theta}$. While many statistical methods have been proposed to compute approximations of $\hat{\theta}$, to our best knowledge, the only statistical method used in movement ecology is the Euler-Maruyama discretization procedure. It is known that the quality of this approximation highly depends on the sampling rate which means that this method might therefore not be well suited to real life animal GPS tags. Therefore, several alternatives are investigated in the following to compute approximations of $\hat{\theta}$. Since all g trajectories are exchangeable, for the sake of clarity, the aforementioned approximation methods will be detailed for a given trajectory and the reference to g is omitted.

Euler-Maruyama method The Euler-Maruyama discretization is an order 0 Taylor expansion of the drift function (as the diffusion coefficient is constant no expansion is required). The drift is therefore assumed to be constant between two observations. For any $0 \leq i \leq n-1$ the target process is approximated by the process $(\mathbf{X}_t^{\text{eul}})_{t_i \leq t < t_{i+1}}$, solution to the SDE: $\mathbf{X}_{t_i}^{\text{eul}} = \mathbf{x}_i$ and, for $t_i \leq t \leq t_{i+1}$,

$$d\mathbf{X}_t^{\text{eul}} = \nabla P_\eta(\mathbf{x}_i) dt + \gamma d\mathbf{W}_t \quad .$$

For all $0 \leq i \leq n-1$, the transition density $q_\theta^{\Delta_i}(\mathbf{x}_i, \mathbf{x}_{i+1})$ is therefore approximated by the transition density of $(\mathbf{X}_t^{\text{eul}})$ between t_i and t_{i+1} denoted by $q_\theta^{\Delta_i, \text{eul}}(\mathbf{x}_i, \mathbf{x}_{i+1})$. This is the probability density of a Gaussian random variable with mean μ_i^{eul} variance Σ_i^{eul} :

$$\begin{aligned} \mu_i^{\text{eul}} &= \mathbf{x}_i + \Delta_i \nabla P_\eta(\mathbf{x}_i) \quad , \\ \Sigma_i^{\text{eul}} &= \begin{pmatrix} \gamma^2 \Delta_i & 0 \\ 0 & \gamma^2 \Delta_i \end{pmatrix} \quad . \end{aligned}$$

Hence, the Euler-Maruyama estimate is given by:

$$\hat{\theta}_{\text{eul}} = \operatorname{argmax}_\theta \prod_{g=1}^G \prod_{i=0}^{n^g-1} q_\theta^{\Delta_i^g, \text{eul}}(\mathbf{x}_i^g, \mathbf{x}_{i+1}^g) \quad . \quad (4)$$

Ozaki method The Ozaki method, proposed in [27] and [30], provides a local linearization of the drift term in order to improve the Euler scheme. For any $0 \leq i \leq n-1$ the target process is approximated by the process $(\mathbf{X}_t^{\text{oz}})_{t_i \leq t < t_{i+1}}$, solution to the SDE: $\mathbf{X}_{t_i}^{\text{oz}} = \mathbf{x}_i$ and, for $t_i \leq t \leq t_{i+1}$,

$$d\mathbf{X}_t^{\text{oz}} = [J_{i,\eta}(\mathbf{X}_t^{\text{oz}} - \mathbf{x}_i) + b_\eta(\mathbf{x}_i)] dt + \gamma d\mathbf{W}_t \quad ,$$

where $J_{i,\eta}$ is the 2×2 Jacobian matrix of the drift function b_η at \mathbf{x}_i . Therefore, the target process is now approximated between each pair of observations by a two-dimensional Ornstein Uhlenbeck process. Then, for all $0 \leq i \leq n-1$, the transition density $q_\theta^{\Delta_i}(\mathbf{x}_i, \mathbf{x}_{i+1})$ is replaced by the transition density of $(\mathbf{X}_t^{\text{oz}})$ between t_i and t_{i+1} denoted by $q_\theta^{\Delta_i, \text{oz}}(\mathbf{x}_i, \mathbf{x}_{i+1})$. If the potential function is such that, for all $0 \leq i \leq n-1$ and all θ , $J_{i,\theta}$ is nonsingular and symmetric (as it is the case of the potential introduced in Section 3.2), following [31], this transition density corresponds to a Gaussian probability density with mean μ_i^{oz} variance Σ_i^{oz} :

$$\begin{aligned} \mu_i^{\text{oz}} &= \mathbf{x}_i + (\exp(J_{i,\eta}) - I_2)(J_{i,\eta})^{-1}b_\eta(\mathbf{x}_i) \quad , \\ \text{vec}(\Sigma_i^{\text{oz}}) &= (J_{i,\eta} \oplus J_{i,\eta})^{-1} (e^{(J_{i,\eta} \oplus J_{i,\eta})\Delta_i} - I_2) \text{vec}(\gamma^2 I_2) \quad , \end{aligned}$$

where I_2 denotes the 2×2 identity matrix, vec is the stack operator and \oplus is the Kronecker sum. The local linearization estimate is then given by:

$$\hat{\theta}_{\text{oz}} = \underset{\theta}{\text{argmax}} \prod_{g=1}^G \prod_{i=0}^{n^g-1} q_\theta^{\Delta_i, \text{oz}}(\mathbf{x}_i^g, \mathbf{x}_{i+1}^g) \quad . \quad (5)$$

Adaptive Kessler method This procedure, proposed in [24], generalizes the Euler-Maruyama method using a higher order approximation of the transition density. Following the same steps as Euler or Ozaki discretizations, [24] proposed to consider a Gaussian approximation of the transition density between consecutive observations. The procedure aims at replacing $q_\theta^{\Delta_i}(\mathbf{x}_i, \mathbf{x}_{i+1})$ by a Gaussian probability density function with mean and variance given by the posterior mean μ_i^{target} and variance Σ_i^{target} of the target process at time t_{i+1} conditionally on the value of the target process at time t_i . This would lead to an approximation with the same two first moments as the target transition density. This approximation can be written similarly to the previous discretization schemes by defining, for any $0 \leq i \leq n-1$, the process $(\mathbf{X}_t^{\text{target}})_{t_i \leq t < t_{i+1}}$ as the solution to the SDE: $\mathbf{X}_{t_i}^{\text{target}} = \mathbf{x}_i$ and, for $t_i \leq t \leq t_{i+1}$,

$$d\mathbf{X}_t^{\text{target}} = \frac{\mu_i^{\text{target}} - \mathbf{x}_i}{\Delta_i} dt + \left(\frac{\Sigma_i^{\text{target}}}{\Delta_i} \right)^{1/2} d\mathbf{W}_t \quad .$$

However, the transition density of the target process being unknown, the conditional expectations μ_i^{target} and Σ_i^{target} are not available in closed form so that [24] proposed to replace these quantities by approximations based on Taylor expansions of these two conditionnal moments (see [19], [24] or [34] for the multidimensionnal case). The transition density $q_\theta^{\Delta_i}(\mathbf{x}_i, \mathbf{x}_{i+1})$ is therefore approximated by the transition density of $(\mathbf{X}_t^{\text{kes}})$ between t_i and t_{i+1} obtained by this expansion and denoted by $q_\theta^{\Delta_i, \text{kes}}(\mathbf{x}_i, \mathbf{x}_{i+1})$. These expansions can be computed directly from the drift and diffusion functions and their partial derivatives. The order of the expansion of the true conditional moments is left to the user and the performance of the estimator highly depends on this parameter, order one being the Euler-Maruyama method. In this paper, it was performed up to the second order. In this case, and for the process defined by (1) and (2), the function $q_\theta^{\Delta_i, \text{kes}}(\mathbf{x}_i, \mathbf{x}_{i+1})$ is the probability density function of a Gaussian random variable with mean μ_i^{kes} variance Σ_i^{kes} (see Proposition 1 of [34] for general formulas):

$$\begin{aligned} \mu_i^{\text{kes}} &= \mathbf{x}_i + \Delta_i \nabla P_\eta(\mathbf{x}_i) \quad , \\ \Sigma_i^{\text{kes}} &= \gamma^2 \Delta_i (I_2 + \Delta_i J_{i,\eta}) \quad . \end{aligned} \quad (6)$$

One can note here that $\mu_i^{\text{kes}} = \mu_i^{\text{eul}}$. A drawback of this method is the fact that (6) does not necessarily define a positive semi-definite matrix. For instance, if $\text{Tr}(J_{i,\eta}) < -2/\Delta_i$, then $\text{Tr}(\Sigma_i^{\text{kes}}) < 0$, which is likely to occur when Δ_i is large. In the following applications, whenever

Σ_i^{kes} is not positive definite, the associated observation is thrown out from the computation of the likelihood, as proposed in [22]. The Kessler estimate is given by:

$$\hat{\theta}_{\text{kes}} = \operatorname{argmax}_{\theta} \prod_{g=1}^G \prod_{i=0}^{n^g-1} q_{\theta}^{\Delta_i^g, \text{kes}}(\mathbf{x}_i^g, \mathbf{x}_{i+1}^g) . \quad (7)$$

It is worth noting here that for numerical stability, equation (6) is not directly plugged into (7), but is replaced by the Taylor expansion of its inverse and its determinant (the resulting contrast function to optimize in multidimensional case is given in [34], p. 2889). In this work, instead of performing direct optimization, the adaptative estimator proposed in [34] is used. This adaptative method provides more numerical stability by alternatively estimating γ and η , (see [34] for details).

Exact Algorithm based Monte Carlo EM method The exact algorithm method proposed by [6] does not rely on Gaussian approximations of the transition densities to compute the maximum likelihood estimator. Details of the method are given in [6] and the important results for the experiments are given in the appendix. Applying the exact algorithm to estimate θ requires the target SDE to be reducible to a unit diffusion using the Lamperti transform which is obtained in our case by setting $(\mathbf{Y}_t := \gamma^{-1}\mathbf{X}_t)_{0 \leq t \leq T}$. Then,

$$d\mathbf{Y}_t = \alpha_{\theta}(\mathbf{Y}_t)dt + d\mathbf{W}_t \quad \text{where} \quad \alpha_{\theta}(\cdot) := \gamma^{-1}b_{\eta}(\gamma \cdot) = \gamma^{-1}\nabla P_{\eta}(\gamma \cdot) . \quad (8)$$

Then, EA1 of [6] relies on the following assumptions.

- *Conservative assumption*: for all $\theta = (\eta, \gamma) \in \mathbb{R}^{d+1}$, there exists $H_{\theta} : \mathbb{R}^2 \mapsto \mathbb{R}$ such that for all $x \in \mathbb{R}^2$,

$$\alpha_{\theta}(x) = \nabla H_{\theta}(x) . \quad (9)$$

- *Boundedness condition*: for all $\theta \in \mathbb{R}^{d+1}$, there exist m_{θ}, M_{θ} , such that for all $x \in \mathbb{R}^2$,

$$m_{\theta} \leq \|\alpha_{\theta}(x)\|^2 + \Delta H_{\theta}(x) \leq M_{\theta} , \quad (10)$$

where Δ is the Laplace operator:

$$\Delta H_{\theta} : x \mapsto \frac{\partial \alpha_{\theta,1}}{\partial x_1}(x) + \frac{\partial \alpha_{\theta,2}}{\partial x_2}(x) .$$

Both conditions are somehow restrictive in general, however, the first one turns out to be satisfied automatically for potential based models studied in ecology, which actually rely on this assumption. The second condition can be relaxed at the cost of additional computations, which is the point of EA2 and EA3 [6]. These algorithms are not studied in this paper as the potential function introduced in Section 3.2 satisfies the boundedness condition. In the case where (9) and (10) hold, we briefly recall the outline of the method.

Let \mathbb{Q}_T^{θ} be the law of $(\mathbf{Y}_t)_{0 \leq t \leq T}$ on $(\mathcal{C}, \mathcal{C})$ when the SDE is parameterized by θ . By the Girsanov formula, \mathbb{Q}_T^{θ} is absolutely continuous with respect to the Wiener measure \mathbb{W}_T on $(\mathcal{C}, \mathcal{C})$ and its Radon-Nikodym derivative is given by:

$$\ell(\omega, \theta) := \log \frac{d\mathbb{Q}_T^{\theta}}{d\mathbb{W}_T}(\omega) = H_{\theta}(\omega_T) - H_{\theta}(\omega_0) - \frac{1}{2} \int_0^T [\Delta H_{\theta}(\omega_s) + \|\alpha_{\theta}(\omega_s)\|^2] ds . \quad (11)$$

The integral in this likelihood ratio cannot be computed as $\mathbf{Z} = \{(\mathbf{Y}_t)_{0 \leq t \leq T}\}$ is not available, only discrete time observations are known. The Expectation Maximization algorithm provides a solution to maximize the likelihood in this incomplete data framework. Starting with

an initial estimate θ_0 , the EM algorithm produces iteratively a sequence $(\theta_p)_{p \geq 0}$ such that the observed likelihood increases at every iteration. Under mild assumptions on the model, $(\theta_p)_{p \geq 0}$ converges to a critical point of the likelihood function [18]. Each iteration of the EM algorithm proceeds in two steps when γ is known:

- E-step: compute the intermediate quantity $\theta \mapsto Q(\theta, \theta_p) = \mathbb{E}_{\theta_p} [\ell(\mathbf{Y}, \theta) | \mathbf{Y}_0, \dots, \mathbf{Y}_n]$, where \mathbb{E}_{θ_p} is the conditional expectation under the law of the process $(\mathbf{Y}_t)_{0 \leq t \leq T}$ given $(\mathbf{Y}_0, \dots, \mathbf{Y}_n)$ when the SDE is parameterized by θ_p .
- M-step: set θ_{p+1} as one maximizer of $\theta \mapsto Q(\theta, \theta_p)$.

The procedure when γ is unknown follows similar steps with additional technicalities and is given in [6]. The intermediate quantity $\theta \mapsto Q(\theta, \theta_p)$ of the EM algorithm might be written as a sum over all segments $[t_{j-1}, t_j]$ of the following expectations:

$$\mathbb{E}_{\theta_p} \left[\int_{t_{j-1}}^{t_j} [\Delta H_\theta(\mathbf{Y}_s) + \|\alpha_\theta(\mathbf{Y}_s)\|^2] ds \middle| \mathbf{Y}_{j-1}, \mathbf{Y}_j \right] .$$

As noted by [6], a nice property is that this quantity reduces to the expectation of the form:

$$\int_{t_{j-1}}^{t_j} [\Delta H_\theta(\mathbf{Y}_s) + \|\alpha_\theta(\mathbf{Y}_s)\|^2] ds = (t_j - t_{j-1}) \mathbb{E}_{\theta_p} [\Delta H_\theta(\mathbf{Y}_{U_j}) + \|\alpha_\theta(\mathbf{Y}_{U_j})\|^2 | (\mathbf{Y}_t)_{t_{j-1} \leq t \leq t_j}] ,$$

where U_j is independent of $(\mathbf{Y}_t)_{t_{j-1} \leq t \leq t_j}$ and uniformly distributed on $[t_{j-1}, t_j]$. Then, the quantity $Q(\theta, \theta_p)$ may be rewritten as

$$Q(\theta, \theta_p) = \mathbb{E}_{\theta_p} [\mathbb{E}_{\theta_p} \{ \Delta H_\theta(\mathbf{Y}_{U_j}) + \|\alpha_\theta(\mathbf{Y}_{U_j})\|^2 | (\mathbf{Y}_t)_{t_{j-1} \leq t \leq t_j} \} | \mathbf{Y}_{j-1}, \mathbf{Y}_j] ,$$

and may be approximated using Monte Carlo simulations using N_j simulations for the expectation over all possible trajectories between \mathbf{Y}_{j-1} and \mathbf{Y}_j and M_j terms for the expectation over the random times U_j .

For all $1 \leq j \leq n$ and all $1 \leq i \leq N_j$,

- (i) simulate $(U_k^{j,i})_{1 \leq k \leq M_j}$ independently and uniformly on $[t_{j-1}, t_j]$;
- (ii) conditional on \mathbf{Y}_{j-1} and \mathbf{Y}_j , sample a skeleton $\mathbf{Y}^{j,i}$ at time instances $(U_k^{j,i})_{1 \leq k \leq M_j}$.

Then, $Q(\theta, \theta_p)$ is estimated by $Q^N(\theta, \theta_p)$ where

$$Q^N(\theta, \theta_p) := H_\theta(\mathbf{Y}_n) - H_\theta(\mathbf{Y}_0) - \frac{1}{2} \sum_{j=1}^n \frac{t_j - t_{j-1}}{M_j N_j} \sum_{i=1}^{N_j} \sum_{k=1}^{M_j} \left\{ \Delta H_\theta(\mathbf{Y}_{U_k^{j,i}}^{j,i}) + \left\| \alpha_\theta(\mathbf{Y}_{U_k^{j,i}}^{j,i}) \right\|^2 \right\} .$$

The procedure to sample each instances of $\mathbf{Y}^{j,i}$ given \mathbf{Y}_{j-1} and \mathbf{Y}_j is the Exact Algorithm EA1 of [6]. This EM based method offers the advantage of avoiding approximation error due to time discretization of the SDE. The only error comes from the Monte Carlo simulations based on M_j, N_j , $1 \leq j \leq n$, used to approximate the expectation in the E-step. In theory, if the conditions (9) and (10) are satisfied, it is always possible to simulate a point \mathbf{Y}_t at any time $t_i \leq t \leq t_{i+1}$ conditionally on the observations \mathbf{Y}_i and \mathbf{Y}_{i+1} . However, the simulation algorithm is based on rejection sampling and the acceptance probability is equal to:

$$\exp \left\{ -\frac{1}{2} (M_\theta - m_\theta) \int_{t_i}^{t_{i+1}} \phi_\theta(\mathbf{Y}_s) ds \right\} , \quad (12)$$

where m_θ and M_θ are defined as in (10), and $\phi_\theta(x) := (\|\alpha_\theta(x)\|^2 + \Delta H_\theta(x) - m_\theta)/2 \geq 0$. Then, the integral in (12) increases with the sampling step, and the acceptance probability decreases to 0. Therefore, the computational complexity of the EA algorithm highly depends on the sampling step.

Approximating the log likelihood The associated loglikelihood of two given estimates $\hat{\theta}_1$ and $\hat{\theta}_2$ cannot be computed exactly. However, in the case where equations (9) and (10) hold, and following [5], an unbiased estimator ℓ_{EA} of the loglikelihood based on Monte Carlo simulations may be computed. This estimator has no intrinsic bias as the error only comes from the Monte Carlo procedure. This allows to choose between two given estimates $\hat{\theta}_1$ and $\hat{\theta}_2$ the one with the greatest likelihood.

3 Estimation of a movement model in ecology

3.1 Form of the potential function

The potential based model proposed in this section is an extension of the models proposed by [29]. The position process of an individual is assumed to satisfy (1) and (2), with a Gaussian shaped potential function of the form:

$$P_\eta(x) = \sum_{i=1}^K \pi_k \varphi_k^\eta(x) \quad \text{where} \quad \varphi_k^\eta(x) := \exp \left\{ -\frac{1}{2} (x - \mu_k)^T C_k (x - \mu_k) \right\} \quad , \quad (13)$$

where:

- K is the number of components of the mixture.
- $\pi_k \in \mathbb{R}^+$ is the relative weight of the k -th component, with $\sum_{k=1}^K \pi_k = 1$.
- $\mu_k \in \mathbb{R}^2$ is the center of the k -th component.
- $C_k \in \mathcal{S}_2^+$ is the the information matrix of the k -th component, where \mathcal{S}_2^+ is the set of 2×2 symmetric positive definite matrices.

In this work, K is assumed to be known and

$$\eta = \{(\pi_k)_{k=1, \dots, K-1}, (\mu_k)_{k=1, \dots, K}, (C_k)_{k=1, \dots, K}\} \in \mathbb{R}^{6K} \quad .$$

The process solution to the SDE (1) and (2) with the potential function (13) has no explicit transition density so that approximate maximum likelihood procedures such as the methods presented in Section 1 may be considered. This specific parametric form of P_η ensures that equations (9) and (10) hold (see the appendix) and therefore, the EA1 algorithm may be used with:

$$H_\theta : x \mapsto \sum_{k=1}^K \pi_k \varphi_k^\eta(\gamma x) / \gamma \quad , \quad (14)$$

with $\theta = (\eta, \gamma)$.

3.2 Simulation study

Simulation design The performance of the four estimation methods presented in this paper is evaluated on a given set of parameters θ and different sampling schemes. The hidden potential map have $K = 2$ components, leading to 12 parameters to estimate, and is represented on Figure 1a. All simulated trajectories start from a common starting point \mathbf{x}_0 and are sampled from the true distribution of the process $(X_t)_{t \geq 0}$ using the accept rejection procedure proposed in [7]. $G = 10$ independent trajectories are simulated with $n_g = 500$ recorded points. Three different sampling time steps are considered, respectively with high

frequency ($\Delta = 0.1$), intermediate frequency ($\Delta = 1$) and low frequency ($\Delta = 10$). In an actual sampling design, this would correspond to three different GPS tags settings with a limited number of emissions (here, 500). In order to evaluate uncertainty of estimation for each method in each scenarios, this procedure is repeated independently with 30 different data sets. For each sampling time step, a 10 trajectory data set is presented on Figure 1. All techniques require a maximization procedure, either for a direct estimation, see (4), (5) and (7), or for the M-step of the EM algorithm. This maximization step is performed using the CMA-ES algorithm proposed by [20]. For each estimation method, 30 initial parameters θ_0 are used and the parameter estimate with the maximum objective function is therefore considered as the estimator $\hat{\theta}$.

Results Figures 2, 3 and 4 provide the estimation of the parameters for the three sampling cases. The best estimation for all parameters and techniques is obtained with the intermediate frequency sampling rate. As illustrated by Figure 1, this frequency allows a good exploration of the map by the process with 500 observations and the different gaussian approximations are satisfactory while the acceptance rate for the EA method remains reasonable. Indeed, the acceptance rate for the three samplings decrease for conditionnal simulation (using the MLE) decreases from 99.6% ($\Delta = 0.1$) to 97.6 ($\Delta = 1$) and 67.5% ($\Delta = 10$) respectively. On the other hand, when $\Delta = 0.1$ with only 500 observations per trajectory, the time horizon 50 might be insufficient for a good parameter estimation using this model. When $\Delta = 10$, there is a strong bias in the estimation of the shape parameters $C^k, k = 1, 2$, and the diffusion coefficient for all methods.

Overall, the quality of the estimation using Euler method seems to decrease drastically with the time step, whereas the three other methods are more robust, for this model and this data set, to the sampling frequency. The Ozaki and Adaptive Kessler method provide similar results to the EA MCEM method, and therefore, in this case, give a good approximation of the maximum likelihood estimator. It is worth noting that the computation cost of the EA MCEM method is much larger, and therefore, might not be recommended in this case.

Figure 5 displays the absolute estimation errors $|P_{\hat{\theta}}(x) - P_{\theta_{true}}(x)|$ for each method. The map is produced using the median off all estimated values as a set of parameters. The Euler method performs much poorly than the other methods when $\Delta = 1$ and $\Delta = 10$. Figure 6 shows the distribution of the integrated squared error $\int_{\mathbb{R}^2} |P_{\hat{\eta}}(x) - P_{\eta_{true}}(x)|^2 dx$ for each method, which is consistent with the results of Figure 5. According to this simulation study, we recommend not to use the Euler method and to prefer one of the three others presented in this paper.

3.3 Inferring fishing zones

Delimiting fishing zones of high potential represents a key step in fisheries management, potentially to set up some marine protected areas. In order to illustrate the performance of each method to define such zones using actual GPS data, the model presented in Section 3.1 is fitted on two set of trajectories of two French fishing vessels named V1 and V2. The two sets of trajectories are represented in Figure 7:

- V1 (Black on Figure 7) The data set of vessel 1 is composed of 15 short trajectories with a total of 724 GPS locations and a sampling time step of around 12 minutes, with some irregularities up to 1 hour.
- V2 (Grey on Figure 7) The data set of vessel 2 is composed of 25 trajectories with a total of 3111 GPS locations and an irregular sampling time step mostly between 15 and 50 minutes, with some irregularities up to 4 hours.

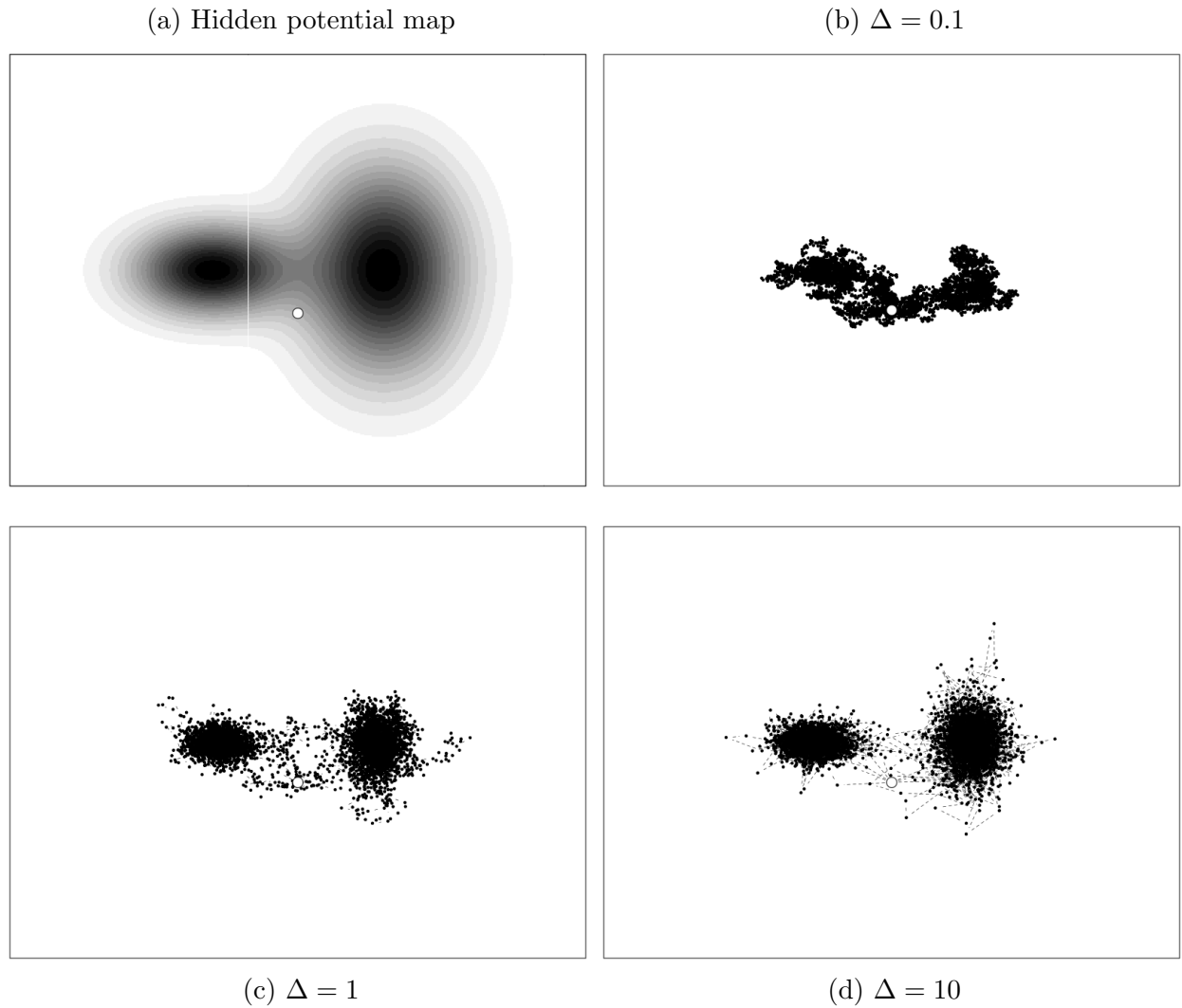


Figure 1: Simulation of the process solution to (1). The potential map driving the movement is shown on Figure 1a. Dark zones present high potential whereas white zones have low potential. The 10 simulated trajectories are sampled 500 times, at three different time steps Δ . The white dot represents the starting point x_0 of each trajectory.

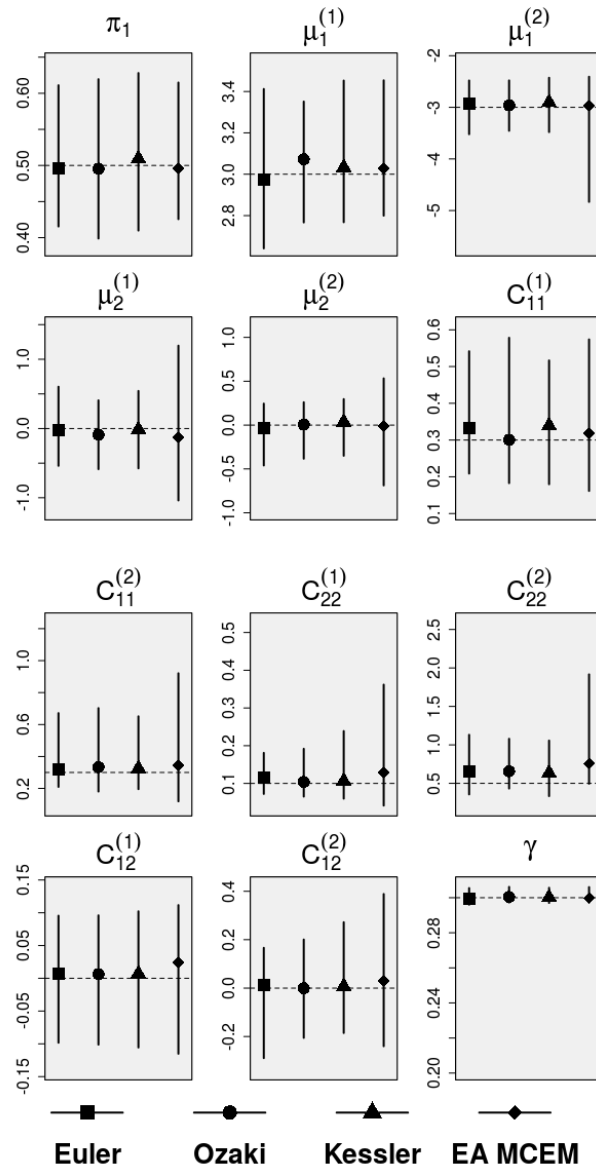


Figure 2: Estimation of the parameters in the case where $\Delta = 0.1$. The dot represents the median, the whiskers provide the 95% range of estimations.

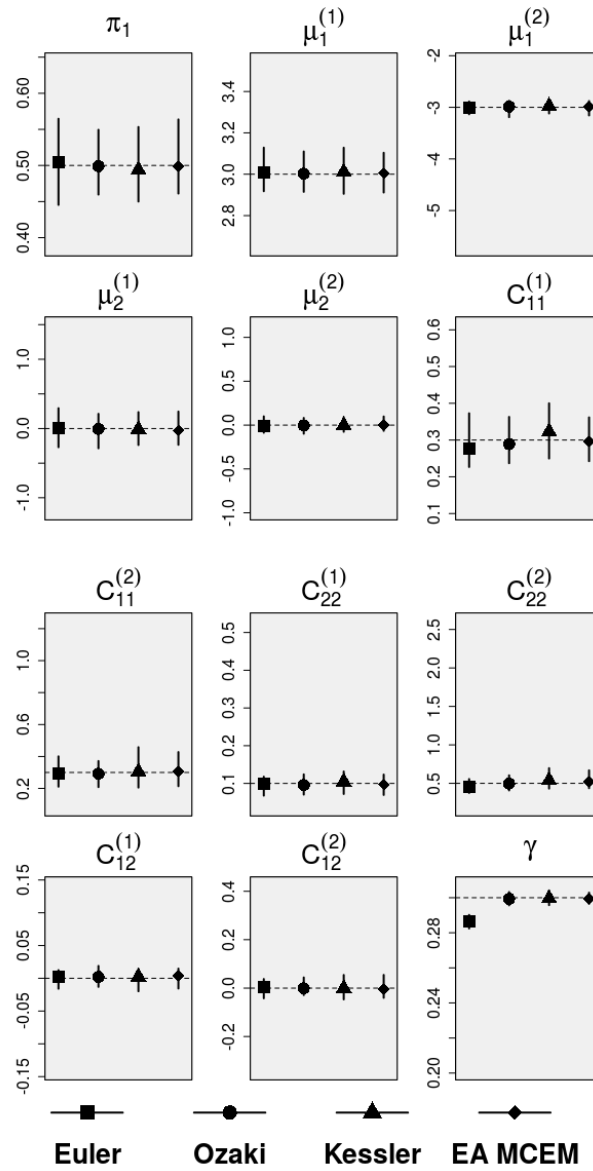


Figure 3: Estimation of the parameters in the case where $\Delta = 1$. The dot represents the median, the whiskers provide the 95% range of estimations.

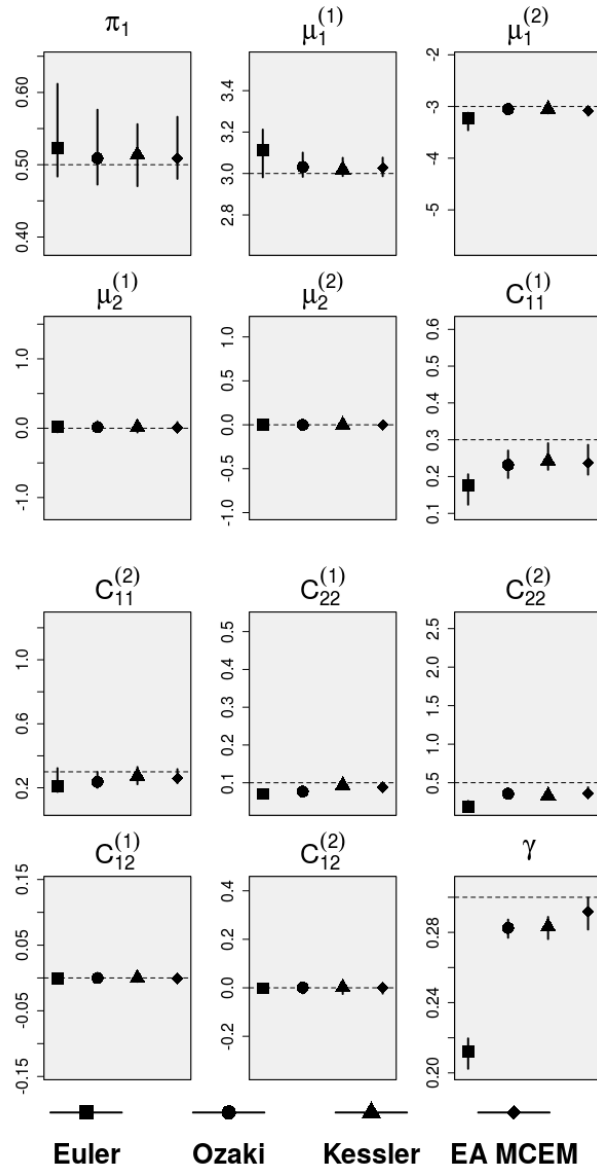


Figure 4: Estimation of the parameters in the case where $\Delta = 10$. The dot represents the median, the whiskers provide the 95% range of estimations.

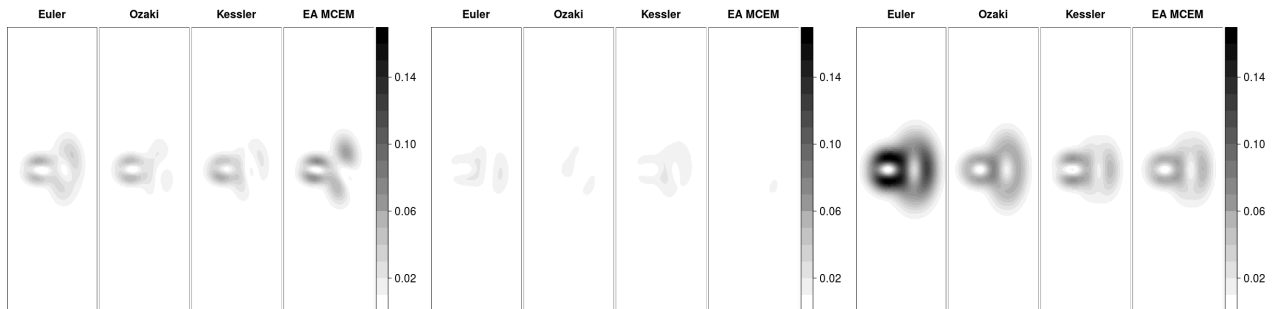


Figure 5: Error between the median map estimate and the true map. Results are presented for each method with $\Delta = 0.1$ (left), 1 (center) and 10 (right).

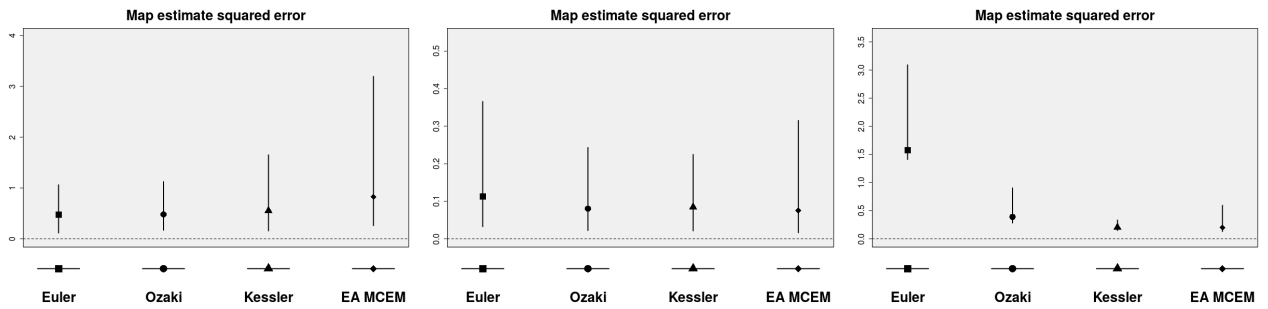


Figure 6: Distribution of the integrated squared error between the estimated map and the true one. Results are presented for each method with $\Delta = 0.1$ (left), 1 (center) and 10 (right).

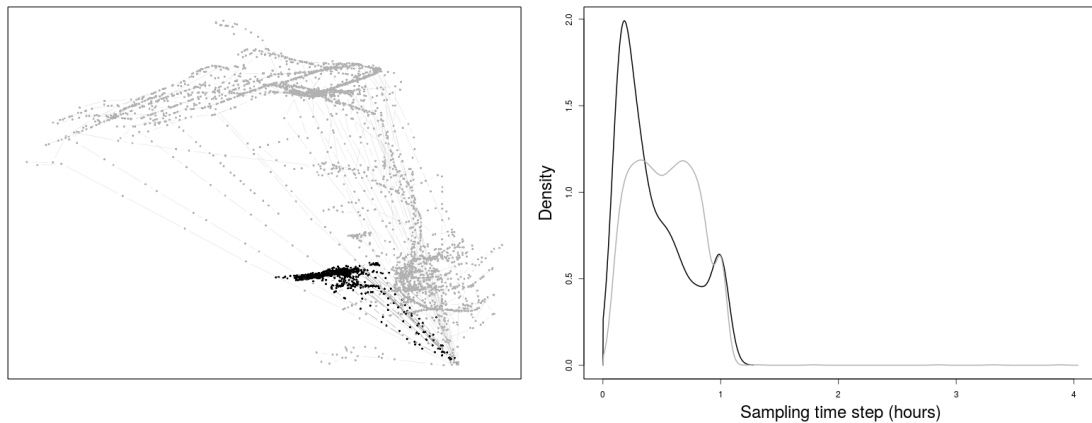


Figure 7: *Left*: The two sets of trajectories are presented with a different color, grey or black, depending on the vessel. *Right*: Distribution of sampling time step for GPS tags are presented for both data sets. Both data set present irregular sampling time step. For confidentiality reason, the actual recorded positions may not be shown and therefore no labels are presented on the axes.

For each data set, the four methods presented above were used to estimate θ . In the model presented in Section 3.1, the number of components K is assumed to be known. In the case of actual data, K has to be estimated. In the presented examples, we do not focus on this problem which has already been addressed in the case of discretely observed SDE (see [33], for instance) and assume $K_1 = 1$ (respectively $K_2 = 3$) for V1 (resp. V2). However, it is worth noting that any model selection based on a penalized likelihood criterion might be approximated as an unbiased approximation of the likelihood has been proposed in [5, Theorem 1]. In the following, this approximation of the likelihood is used to choose which estimation method provides the best estimated map.

Results for V1 Results for the vessel 1 are presented in Figure 8. The best estimate in the sense of the greatest approximated log-likelihood is given by the map estimated with the MCEM EA method, followed by Ozaki, Kessler and Euler (see Table 1 for the values of each log-likelihood, for each estimated parameter). $\hat{\theta}_{\text{kes}}$ is quite unstable, as the correction term for the variance (given in equation (6)) leads to a non positive semi-definite matrix for 28% of the observations. However, the estimated map is similar to the one given by Ozaki and EA MCEM methods although less concentrated around the data. The EA MCEM method provides the best estimate in terms of likelihood. The acceptance rate for conditionnal simulation is of 1.4%. Euler discretization method estimates a potential map with a much more spread attractive zone than the three other methods. Moreover, the orientation of this zone does not follow what seems to be the main axis of trawling (mainly East-West, here). Both Ozaki and MCEM EA methods provide a similar estimated map (it terms of parameters and of likelihood): a Gaussian form wrapping what appears to be the main trawling zone. The axis of the resulting Gaussian form are conform to the trawling directions of the vessels.

Results for V2 Results for the vessel 2 are presented in Figure 9. As in the case of V1, the best estimate in the sense of the greatest approximated loglikelihood is given by the map estimated with the MCEM EA method, followed by Ozaki, Kessler and Euler (see Table 1 for the values of each log-likelihood, for each estimated parameter). Again, $\hat{\theta}_{\text{kes}}$ is unstable, as the correction term for the variance leads to a non positive semi-definite matrix for 48% of observations. The EA MCEM method provides the best estimate in terms of likelihood. The acceptance rate for conditionnal simulation is of 6.2%.

As for vessel 1, Euler method results in a smooth estimated map, where attractive zones are connected, and wrap almost all observed points. Kessler, Ozaki and MCEM EA methods lead to maps where zones are disconnected: one close to to the harbour and an offshore zone. In the case of the Adaptive Kessler method, the extension and the relative weight of this first zone is larger than for the two other methods. For the three methods, the second offshore zone is a mixture of a general attractive zone with an East-West orientation, and a smaller hot spot that gathers a large amount of observed points. Here, a natural extension would be to use larger values for K .

The Gaussian model proposed by [29] would have imposed a potential function whose orientation is given by the x and y axis, with circular contour lines as a consequence of the independence between directions. The generalization proposed in this paper model more complex attractive zones. The contour lines of the potential might be used to define more realistic high potential fishing zones.

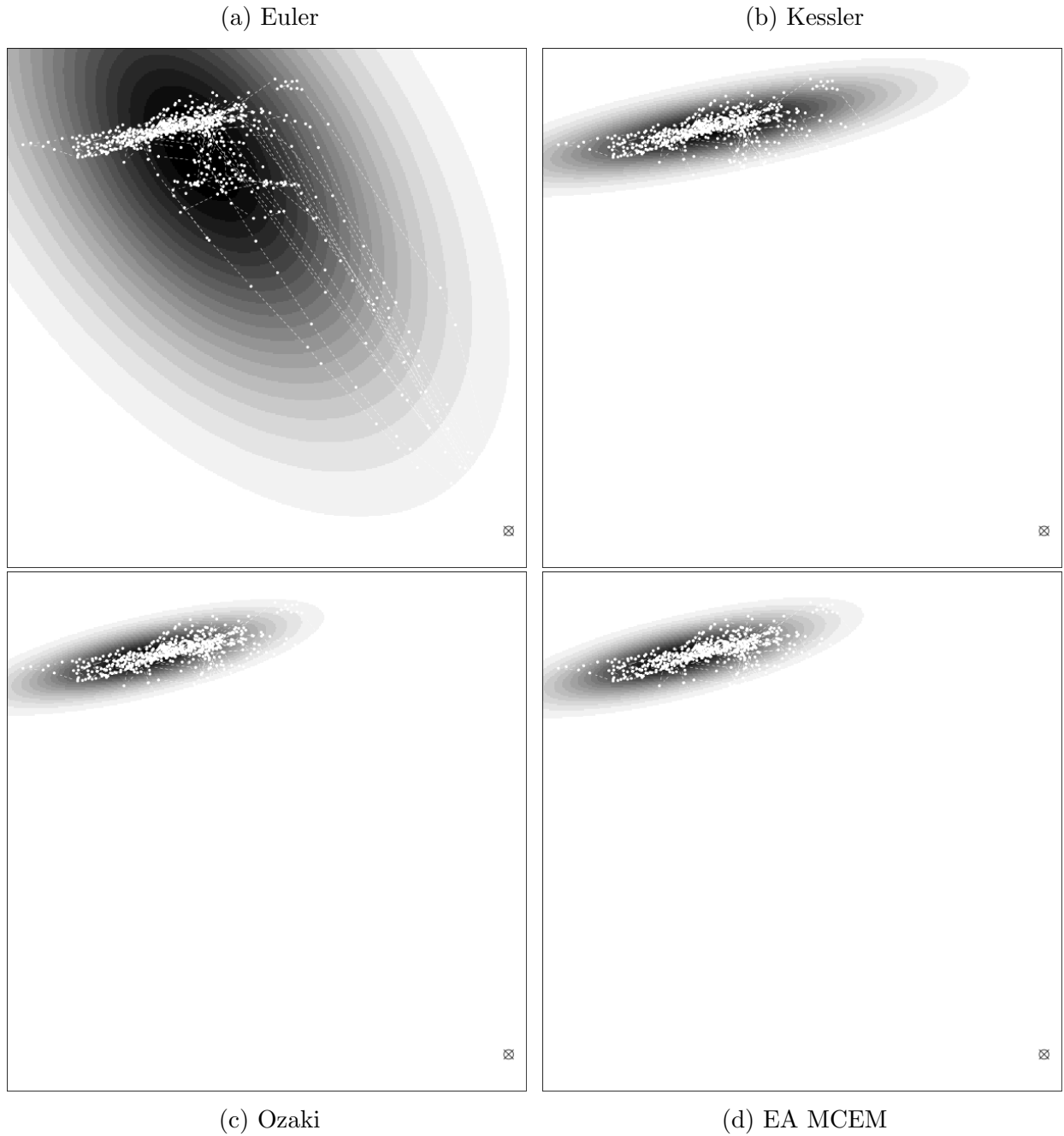


Figure 8: Estimated map for the data set of the vessel 1 (see Figure 7, using four different estimation methods). The cross in the bottom right of each map is the departure harbour. The darker a zone is, the more attractive it is for the given vessel. Observed points, in white, are plotted in order to see the superposition between maps and trajectories.

Estimate \ Criterion	V1				V2			
	ℓ_{Eul}	ℓ_{Oza}	ℓ_{Kes}	ℓ_{EA}	ℓ_{Eul}	ℓ_{Oza}	ℓ_{Kes}	ℓ_{EA}
θ_{Eul}	-1.29	-0.37	-1.29	-1.32	-2.17	-2.16	-1.07	-2.15
θ_{Oza}	-1.50	-0.91	0.39	-0.93	-2.21	-2.09	-0.90	-2.07
θ_{Kes}	-1.50	-0.96	0.70	-0.99	-2.26	-2.18	-0.67	-2.09
θ_{EA}	-1.49	-0.92	0.06	-0.92	-2.21	-2.11	-0.98	-2.06

Table 1: Value of the function to optimize for each estimated parameter, for each data set. Highest value for each column is on the diagonal. Values are normalized contrasts (divided by the number of segments of trajectories).

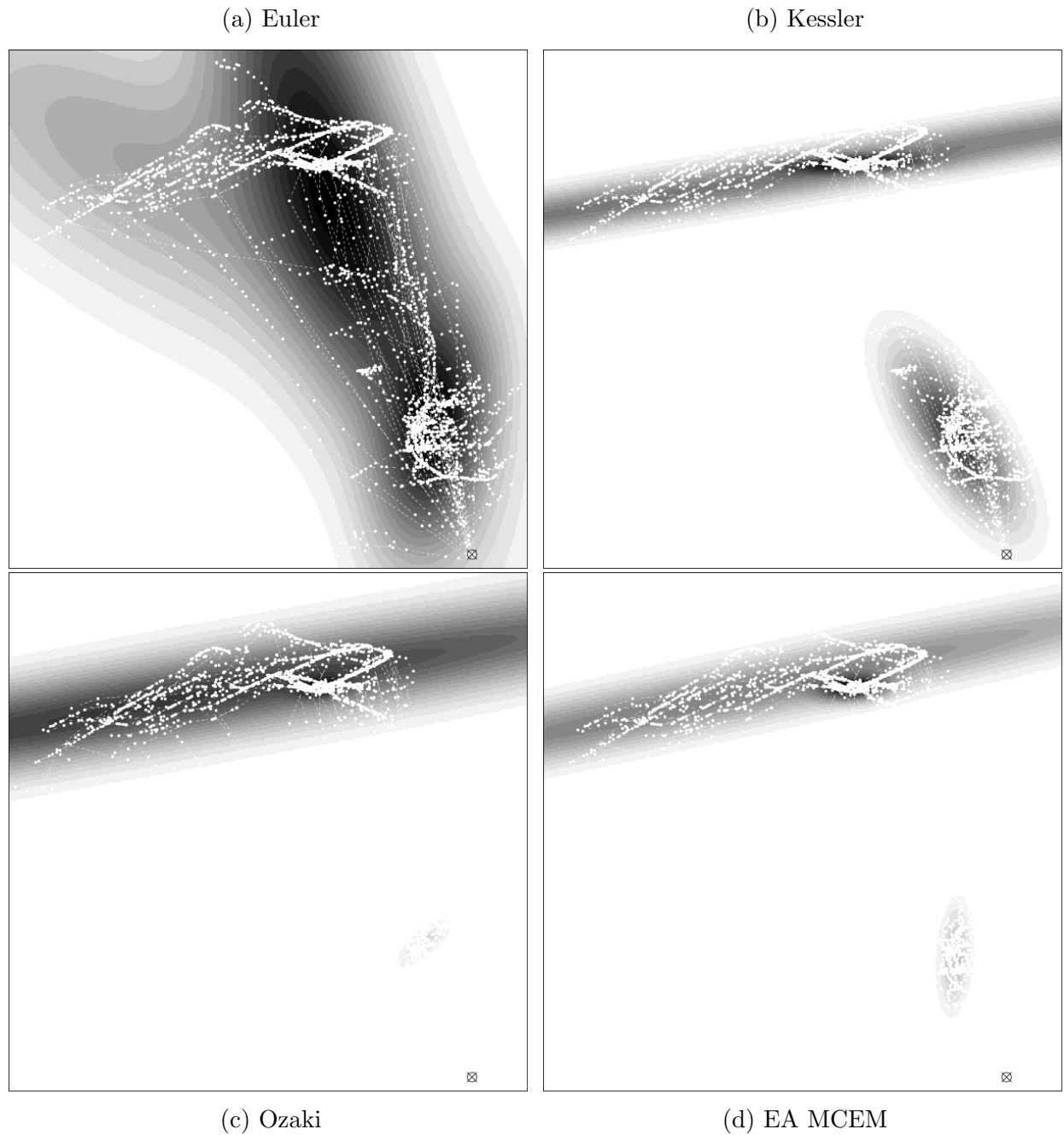


Figure 9: Estimated map for the data set of the vessel 2 (see Figure 7,) using four different estimation methods. The cross in the bottom right of each map is the departure harbour. The darker a zone is, the more attractive it is for the given vessel. Observed points, in white, are plotted in order to see the superposition between maps and trajectories.

4 Conclusions

This paper explores the performance of four inference methods to estimate parameters of a new movement model based on a stochastic differential equation. The drift of this SDE is defined as the gradient of a mixture of smooth potential functions while its diffusion term is constant but unknown. Numerical experiments with simulated and real data illustrate that the Euler discretization method is not robust to low sampling rates, which is a common situation in movement ecology, and that the three other approximate maximum likelihood methods perform better. Two estimation procedures are based on a Gaussian approximation of the likelihood similar to and as easy to implement as the Euler approach. The last method based on a Monte Carlo EM using the Exact Algorithm requires additional mathematical assumptions on the model and is more technically and computationally intensive.

These four methods were compared to estimate potential maps (from a specific model) using actual movement data issued from fishing vessels. Overall, it is clear here that the different methods can lead to different maps with various interpretations. In the case presented here, among the three pseudo likelihood methods, the Ozaki method seems to provide the closest estimate to the one given by the EA MCEM method, which is the best in terms of likelihood. It is worth noting here that this last method is way more difficult to implement, more computationally intensive and its applications are restricted to a specific kind of potential functions. The Ozaki method as presented in this paper is restricted to potentials with invertible Jacobian matrices at observed data points, which is a weaker assumption. The Adaptive Kessler approximate method was more unstable than the Ozaki discretization as the proposed approximation of the covariance matrix can be non positive semi-definite for some observed points. However, the estimation procedure was robust to those points and provided estimates close to the EA MCEM and Ozaki methods. The method is only used in this work with an expansion of conditional moments up to order two and higher order expansions could lead to more robust estimates. Although the Euler method is the most widely used in movement ecology, the two other approximate likelihood procedures exhibit better performances and are as easy to implement. The EA MCEM based method seems the most appealing as it does not introduce any bias but the difficulty of its implementation and the computation cost might reduce its interest.

In addition, several extensions of the proposed potential based model could be considered. If some part of the trajectories can hardly be modeled using SDE (for fishing vessels) we could use a Markov switching SDE where the state might follow several dynamics depending on a regime indicator given by a finite state space hidden Markov chain. The trajectories are not likely to be independent but could also be modeled as the solution to a $2G$ dimensional SDE with interactions in the drift function and the diffusion matrix. As the individuals are not observed at the same time, a partially observed SDE can be defined which implies additional challenges to estimate model parameters using algorithms designed for hidden Markov models. Finally, an undesirable property of the potential introduced in the paper is that, far from the attractive zones, the process behaves like a Brownian motion. This can be easily overcome for instance by adding another component in the mixture proportional to $-\|x - \mu_G\|^{1/2}$, where G is a fixed attractive point. This ensures that even if an individual is far from the attractive zones, he is likely to revert around G . We used this potential and obtained very similar numerical results. We decided not to add this component in the model as it seemed artificial to ensure stationarity for theoretical reasons.

Acknowledgments: The authors would like to thank three anonymous referees for their meaningful comments which led to a major reorientation of this work. Meeting expenses between the three authors have been supported by the GdR EcoStat. The data used in this

work would not have been carried out without all contributors to the RECOPESCA project. The authors express their warm thanks to the leaders of this project Patrick Berthou and Emilie Leblond and all the voluntary fishermen involved in this project. The authors have also benefited from insightful discussions with Valentine Genon-Catalot and Catherine Laredo.

A Applying EA1 to H_θ

Lemma A.1. For all θ and all $x \in \mathbb{R}^2$,

$$0 \leq \|\alpha_\theta(x)\|^2 \leq \bar{\alpha}_\theta \quad ,$$

where α_θ is given by (9) and (14), with $\lambda_1^{(k)}$ and $\lambda_2^{(k)}$ the eigenvalues of C_k , $1 \leq k \leq K$,

$$\bar{\alpha}_\theta := e^{-1} \gamma^{-2} \bar{\pi} \sum_{k=1}^K \pi_k \max_{1 \leq j \leq 2} \lambda_j^{(k)} \quad \text{and} \quad \bar{\pi} := \sum_{k=1}^K \pi_k \quad . \quad (15)$$

Proof. For all θ and all $x \in \mathbb{R}^2$, by convexity of $\|\cdot\|^2$,

$$\begin{aligned} \|\alpha_\theta(x)\|^2 &= \left\| \sum_{k=1}^K \pi_k \varphi_k(\gamma x) \gamma^{-1} C_k (\gamma x - \mu_k) \right\|^2 \quad , \\ &\leq \bar{\pi} \sum_{k=1}^K \pi_k \varphi_k^2(\gamma x) \left\| \gamma^{-1} C_k (\gamma x - \mu_k) \right\|^2 \quad , \\ &\leq \bar{\pi} \sum_{k=1}^K \pi_k \gamma^{-2} \|C_k (\gamma x - \mu_k)\|^2 \exp\left(-(\gamma x - \mu_k)^T C_k (\gamma x - \mu_k)\right) \quad . \end{aligned}$$

Let Λ_k be defined by $C_k = P_k^{-1} \Lambda_k P_k$ where Λ_k is the diagonal matrix with diagonal given by $(\lambda_1^{(k)}, \lambda_2^{(k)})$ and where $P_k P_k^T = I_2$. If $z_k := P_k (\gamma x - \mu_k)$ then,

$$\|\alpha_\theta(x)\|^2 \leq \bar{\pi} \gamma^{-2} \sum_{k=1}^K \pi_k \underbrace{z_k^T \Lambda_k^2 z_k \exp\left(-[z_k^T \Lambda_k z_k]\right)}_{f(z_k)} \quad ,$$

where we used $\|P_k^T z_k\|^2 = \|z_k\|^2$ as P_k is orthogonal. The proof is concluded upon noting that for all $x \in \mathbb{R}^2$,

$$f(x) \leq e^{-1} \max_{1 \leq j \leq 2} \lambda_j^{(k)} \quad .$$

□

Lemma A.2. For all θ and all $x \in \mathbb{R}^2$,

$$\Delta_\theta^- \leq \Delta H_\theta(x) \leq \Delta_\theta^+ \quad ,$$

where H_θ is given by (14) and, with $\lambda_1^{(k)}$ and $\lambda_2^{(k)}$ the eigenvalues of C_k , $1 \leq k \leq K$,

$$\Delta_\theta^- := - \sum_{k=1}^K \pi_k \text{Tr}(C_k) \quad , \quad (16)$$

$$\Delta_\theta^+ := 2e^{-1} \sum_{k=1}^K \pi_k \max_{1 \leq j \leq 2} \lambda_j^{(k)} \quad . \quad (17)$$

Proof. By equation (14), if Tr denotes the Trace operator,

$$\begin{aligned}
\Delta H_\theta(X) &= \text{Tr} [\nabla \alpha_\theta(x)] \quad , \\
&= -\text{Tr} \left[\nabla \left(\sum_{k=1}^K \pi_k \varphi_k(\gamma x) \gamma^{-1} C_k (\gamma x - \mu_k) \right) \right] \quad , \\
&= -\text{Tr} \left[\sum_{k=1}^K \left(\pi_k \nabla \varphi_k(\gamma x) \gamma^{-1} [C_k (\gamma x - \mu_k)]^T + \pi_k \varphi_k(\gamma x) \gamma^{-1} C_k \gamma \right) \right] \quad , \\
&= -\sum_{k=1}^K \pi_k \varphi_k(\gamma x) \left\{ -\text{Tr}([C_k (\gamma x - \mu_k)] [C_k (\gamma x - \mu_k)]^T) + \text{Tr}(C_k) \right\} \quad , \\
&= \underbrace{\sum_{k=1}^K \pi_k \varphi_k(\gamma x) \|C_k (\gamma x - \mu_k)\|^2}_{I(x)} - \underbrace{\sum_{k=1}^K \pi_k \varphi_k(\gamma x) \text{Tr}(C_k)}_{J(x)} \quad .
\end{aligned}$$

By definition of φ_k , for all $1 \leq k \leq K$,

$$0 \leq J(x) \leq \underbrace{\sum_{k=1}^K \pi_k \text{Tr}(C_k)}_{-\Delta_\theta^-} \quad .$$

Following the same steps as for the proof of Lemma A.1,

$$0 \leq I(x) \leq \underbrace{2e^{-1} \sum_{k=1}^K \pi_k \max_{1 \leq j \leq 2} \lambda_j^{(k)}}_{\Delta_\theta^+} \quad .$$

□

References

- [1] Y. Ait-Sahalia. Transition densities for interest rate and other nonlinear diffusions. *Journal of Finance*, 54:1361–1395, 1999.
- [2] Y. Ait-Sahalia. Maximum likelihood estimation of discretely sampled diffusions: a closed-form approximation approach. *Econometrica*, 70:223–262, 2002.
- [3] Y. Ait-Sahalia. Closed-form likelihood expansions for multivariate diffusions. *The Annals of Statistics*, 36:906–937, 2008.
- [4] A. Beskos, O. Papaspiliopoulos, and G. Roberts. Retrospective exact simulation of diffusion sample paths with applications. *Bernoulli*, 12(6):1077–1098, 2006.
- [5] A. Beskos, O. Papaspiliopoulos, and G. Roberts. Monte Carlo maximum likelihood estimation for discretely observed diffusions processes. *Annals of Statistics*, 37(1):223–245, 2009.
- [6] A. Beskos, O. Papaspiliopoulos, G. Roberts, and P. Fearnhead. Exact and computationally efficient likelihood-based estimation for discretely observed diffusion processes. *Journal of Royal Statistical Society, Series B: Statistical Methodology*, 68:333–382, 2006.

- [7] A. Beskos and O. Roberts G. Exact simulation of diffusions. Annals of Applied Probability, 15(4):2422–2444, 2005.
- [8] S. Bestley, I. D. Jonsen, M. A. Hindell, R. G. Harcourt, and N. J. Gales. Taking animal tracking to new depths: synthesizing horizontal–vertical movement relationships for four marine predators. Ecology, 96(72):417–427, 2015.
- [9] P. Blackwell. Random diffusion models for animal movement. Ecological Modelling, 100(1–3):87 – 102, 1997.
- [10] P. Blackwell, M. Niu, M. Lambert, and S. LaPoint. Exact Bayesian inference for animal movement in continuous time. Methods in Ecology and Evolution, 2015.
- [11] D. Brillinger. Handbook of Spatial Statistics, chapter 26. Chapman and Hall/CRC Handbooks of Modern Statistical Methods. CRC Press, 2010.
- [12] D. Brillinger, K. Haiganoush, A. Ager, J. Kie, and B. Stewart. Employing stochastic differential equations to model wildlife motion. Bulletin of the Brazilian Mathematical Society, 33:385–408, 2002.
- [13] D. Brillinger, H. Preisler, A. Ager, and J. Kie. The use of potential functions in modeling animal movement. Data analysis from statistical foundations, pages 369–386, 2001.
- [14] D. Brillinger, H. Preisler, A. Ager, J. Kie, and B. Stewart. Modeling movements of free-ranging animals. Univ. Calif. Berkeley Statistics Technical Report, 610, 2001.
- [15] D. Brillinger, H. Preisler, and M. Wisdom. Modeling particles moving in a potential field with pairwise interactions and an application. Brazilian Journal of Probability and Statistics, 25(3):421–436, 2011.
- [16] S.-K. Chang. Application of a vessel monitoring system to advance sustainable fisheries management—Benefits received in Taiwan. Marine Policy, 35(2):116–121, 2011.
- [17] A. S. G. E. M. Chavez. Landscape Use and Movements of Wolves in Relation to Livestock in a Wildland–Agriculture Matrix. Journal of Wildlife Management, 70(4):1079–1086, 2006.
- [18] A. P. Dempster, N. M. Laird, and D. B. Rubin. Maximum likelihood from incomplete data via the EM algorithm. J. Roy. Statist. Soc. B, 39(1):1–38 (with discussion), 1977.
- [19] D. Florens-zmirou. Approximate discrete-time schemes for statistics of diffusion processes. Statistics, 20(4):547–557, 1989.
- [20] N. Hansen and A. Ostermeier. Completely derandomized self-adaptation in evolution strategies. Evolutionary Computation, 9(2):159–195, 2001.
- [21] K. J. Harris and P. G. Blackwell. Flexible continuous-time modeling for heterogeneous animal movement. Ecological Modelling, 255:29–37, APR 24 2013.
- [22] S. M. Iacus. Simulation and inference for stochastic differential equations: with R examples, volume 1. Springer Science & Business Media, 2009.
- [23] D. Johnson, J. London, M.-A. Lea, and J. Durban. Continuous-time correlated random walk model for animal telemetry data. Ecology, 89(5):1208–1215, 2008.

- [24] M. Kessler. Estimation of an ergodic diffusion from discrete observations. Scandinavian Journal of Statistics, 24(2):211–229, 1997.
- [25] M. Kessler, A. Lindner, and M. Sorensen. Statistical methods for stochastic differential equations. CRC Press, 2012.
- [26] C. Li. Maximum-likelihood estimation for diffusion processes via closed-form density expansions. The Annals of Statistics, 41(3):1350–1380, 2013.
- [27] T. Ozaki. A bridge between nonlinear time series models and nonlinear stochastic dynamical systems: a local linearization approach. Statistica Sinica, pages 113–135, 1992.
- [28] H. Preisler, A. Ager, B. Johnson, and J. Kie. Modeling animal movements using stochastic differential equations. Environmetrics, 15(7):643–657, 2004.
- [29] H. Preisler, A. Ager, and M. Wisdom. Analyzing animal movement patterns using potential functions. Ecosphere, 4(3), 2013.
- [30] I. Shoji and T. Ozaki. Estimation for nonlinear stochastic differential equations by a local linearization method 1. Stochastic Analysis and Applications, 16(4):733–752, 1998.
- [31] I. Shoji and T. Ozaki. A statistical method of estimation and simulation for systems of stochastic differential equations. Biometrika, 85(1):240–243, 1998.
- [32] J. Skellam. Random dispersal in theoretical populations. Biometrika, pages 196–218, 1951.
- [33] M. Uchida and N. Yoshida. AIC for ergodic diffusion processes from discrete observations. preprint MHF, 12, 2005.
- [34] M. Uchida and N. Yoshida. Adaptive estimation of an ergodic diffusion process based on sampled data. Stochastic Processes and their Applications, 122(8):2885 – 2924, 2012.